

Dalton Transactions

Accepted Manuscript



This is an *Accepted Manuscript*, which has been through the Royal Society of Chemistry peer review process and has been accepted for publication.

Accepted Manuscripts are published online shortly after acceptance, before technical editing, formatting and proof reading. Using this free service, authors can make their results available to the community, in citable form, before we publish the edited article. We will replace this *Accepted Manuscript* with the edited and formatted *Advance Article* as soon as it is available.

You can find more information about *Accepted Manuscripts* in the [Information for Authors](#).

Please note that technical editing may introduce minor changes to the text and/or graphics, which may alter content. The journal's standard [Terms & Conditions](#) and the [Ethical guidelines](#) still apply. In no event shall the Royal Society of Chemistry be held responsible for any errors or omissions in this *Accepted Manuscript* or any consequences arising from the use of any information it contains.

Royal Society of Chemistry

Guidelines to Referees (research works)

Dalton Transactions - www.rsc.org/dalton

Dalton Transactions wishes to encourage very high quality papers reporting exciting new developments in inorganic chemistry and biological inorganic chemistry. For an article to be accepted it must report high quality new chemistry and make a significant contribution to the field - please bear this in mind when making your recommendation - the current Impact Factor of **Dalton Transactions** is 3.83.

Dalton Transactions embraces all aspects of the chemistry of inorganic and organometallic compounds, including biological inorganic and bioinorganic chemistry, organometallics and catalysis, solid-state and coordination chemistry, inorganic materials and the properties and reactions of inorganic compounds.

Routine or unnecessarily fragmented work, however competently researched and reported, should **not** be recommended for publication.

Communications must report high quality new chemistry of sufficient importance and impact to justify preliminary publication.

General Guidance

When preparing your report, please:

- comment on the originality, importance, impact and scientific reliability of the work;
- state unequivocally whether you would like to see the paper accepted or rejected and give detailed comments (with references, as appropriate) that will both help the Editor to make a decision on the paper and the authors to improve it;
- do not make comments about the manuscript or authors which may cause offence.

For confidentiality reasons, please:

- treat the work and the report you prepare as confidential; the work may not be retained (in any form), disclosed, used or cited prior to publication; if you need to consult colleagues to help with the review, please inform them that the manuscript is confidential, and inform the Editor;
- do not communicate directly with authors; *NB* your anonymity as a referee will be strictly preserved from the authors.

Please inform the Editor if:

- there is a conflict of interest;
- there is a significant part of the work which you are not able to referee with confidence;
- if the work, or a significant part of the work, has previously been published, including online publication (e.g. on a preprint server/open access server);
- you believe the work, or a significant part of the work, is currently submitted elsewhere;
- the work represents part of an unduly fragmented investigation.

When submitting your report, please:

- provide your report rapidly and within the specified deadline, or inform the Editor immediately if you cannot do so;
- submit your report at www.rsc.org/referees.

For further details, see the RSC's Refereeing Procedure and Policy — www.rsc.org/pdf/authrefs/ref.pdf

PERSPECTIVE

Computational insights into the photodeactivation dynamics of phosphors for OLEDs: a perspective

Cite this: DOI: 10.1039/x0xx00000x

Daniel Escudero,^{a,*} Denis Jacquemin^{a,b}Received 00th January 2012,
Accepted 00th January 2012

DOI: 10.1039/x0xx00000x

www.rsc.org/

A detailed molecular-level understanding of both the photoluminescence and electroluminescence properties of transition-metal (TM) complexes used as emitters in organic light-emitting diodes (OLEDs) is vital to pave the way to the next generation of OLEDs materials. In this Perspective, we present recent *ab initio* and density-functional theory (DFT) results, including or not spin-orbit couplings (SOCs), focused on disentangling competing photodeactivation mechanisms of radiative and non-radiative nature of target Pt(II) and Ir(III) complexes. These complexes are the most widespread organo-transition metal compounds for OLEDs applications. We address their photodeactivation dynamics, their temperature-dependent photoluminescence kinetics and some unusual photophysical properties (such as e.g. dual photoluminescence or Non-Kasha emissive behaviour). In addition, we discuss the pending questions regarding the photophysics of these systems, which will require the interplay between theoretical and experimental efforts.

I. Introduction

During the last decades an increasing effort has been put into the development of highly efficient electroluminescent devices. In that framework, OLEDs,¹ due to their outstanding optical and electrical properties and their low-cost of fabrication, emerged as excellent candidates. Several strategies have been considered to enhance their electroluminescence efficiency, that are either based on the use of fluorescence, thermally activated delayed fluorescence (TADF)² or phosphorescence. Phosphorescent-based OLEDs (PhOLEDs) can achieve internal electroluminescence quantum efficiencies of almost 100%.³ Notably, Ir(III) and Pt(II) complexes are commonly used as phosphors in PhOLEDs, due to their often exceptional internal quantum efficiencies of phosphorescence, their photostability and the possibility to tune their emission energy from red to blue by adequate chemical modification of their ligands.⁴ Over the past few years, the progress in OLEDs research^{5,6} has been accompanied with the advances in experimental techniques, notably high-resolution and femtosecond time-resolved spectroscopies, such as femtosecond resolved photoluminescence and pump-probe transient absorption spectroscopy.⁷ These techniques enabled to obtain ultrafast electronic/vibrational relaxation information in TM complexes. The ultrafast spin dynamics is typically controlled by the nature and alignment of the singlet and triplet excited state manifolds and the amplitude of their associated SOC. These factors ultimately determine the time-scales of the intersystem crossing (ISC) processes. Hence, for octahedral-like Ir(III) cyclometalated complexes, such as tris(2-phenylpyridine)Ir(III) [Ir(ppy)₃] and tris(1-phenylisoquinoline)Ir(III) [Ir(piq)₃], ISC

processes occur almost quantitatively in less than 100 fs.⁸ Square-planar Pt(II) complexes show more variability in their ISC time-scales, ranging from <50 fs for [Pt(thpy)₂]⁹ (thpy=2-thienylpyridine) to 10-30 ps for the diplatinum complex¹⁰ [Pt₂(P₂O₅H₂)₄]⁴⁺ (PtPOP). Indeed, fluorescence might compete with ISC processes in some Pt(II) complexes.¹¹ Thus, there are no clear trends in ISC rates on the basis of the SOC of the metal atom, since complexes containing lighter metal atoms might exhibit faster ISC rates. Moreover, the photoluminescence properties of these complexes are very often temperature-dependent.¹² Usually, their luminescence efficiency decreases when going from cryogenic conditions to room temperature due to the population of thermally activated triplet metal-centered (³MC) states, which are involved in nonradiative decay channels.¹³ In addition, the temperature might also modulate the radiative rates. TADF is a clear illustration of the importance of the temperature-dependent behaviour of photoluminescence. Likewise, one of us recently described a Non-Kasha emissive behaviour in a cyclometalated Pt(II) complex on the basis of the thermal population of higher-lying triplet excited states,¹⁴ which implies a kinetic control of photoluminescence. Therefore, having in mind that OLEDs should be designed to work at ambient temperatures, controlling the temperature-dependence behaviour is a major factor to account in the design of more efficient phosphors.

Unfortunately, ultrafast spectroscopies cannot, in most of the cases, provide hints into the character, spin and structure of the involved excited states. Towards these aims, excited-state quantum chemical calculations are necessary. From a computational viewpoint, the study of the photophysics and photochemistry of (very often) open-shell TMs remains challenging.¹⁵ However, the recent improvements in *ab initio*

quantum chemical and DFT methods for the excited states of TM complexes¹⁶ extended the applications from a qualitative assignment of absorption and emission processes to a semi-quantitative interpretation of both emission spectroscopy and photochemical reactivity.¹⁷ An additional challenge when modelling phosphors is that their photophysical and photochemical properties are often strongly influenced by the chemical environment (e.g., counterions,¹⁸ solvent,¹⁹ concentration,²⁰ crystal packing effects²¹ or host medium in the emissive layer of an OLED device).²² Hence, not only the photophysical properties might be modulated by the environment (e.g., emission solvent switching²³ and excimer formation²⁴) but also new photodeactivation pathways might appear in the condensed phase, e.g., bimolecular triplet-triplet annihilation (TTA) processes.²⁵ These processes compete with the radiative and non-radiative deactivation pathways and their exploration in the solid phase consequently becomes vital for phosphor modelling.

The objective of this Perspective is not to present an overview of computational methods for the excited states of TM complexes, something that it has been recently reviewed somewhere else,^{15,16} but to present recent computational works performed to unravel the intricate photodeactivation processes occurring in phosphors and to underline the future perspectives in phosphor's research. The choice of those examples is a licence of the authors, driven by our experience and own interests. We apologize for not being able to cite all the important contributions to the field.

II Excited-state computational methods for phosphors

The computational study of the excited states of TM complexes remains difficult as they concentrate most of the complexities inherent to theoretical investigations. Among these, we highlight: multireference character of the excited states, near degeneracies, relativistic effects (importantly SOCs), vibronic couplings, size, environmental effects and multiple excited states of different character [i.e. metal-to-ligand charge transfer (MLCT), MC, ligand-to-ligand charge transfer (LLCT), ligand-centered (LC), metal-to-metal charge transfer (MMCT), among others].^{15,16} Multi-configurational methods, such as the complete-active-space second-order perturbation theory (CASPT2)²⁶ or the restricted-active-space PT2 (RASPT2)²⁷ approaches, are in principle well suited for TM complexes.^{28,29} Indeed, due to the balanced treatment of dynamic and non-dynamic electron correlation, these methods are capable to deal with all kinds of electronic structure. However, they have not yet acquired a "gold standard" status for the spectroscopy and photochemistry of TM complexes, since, on the one hand, their accuracy is critically dependent on their judicious use, particularly with regard to the selection of a chemically-sound active space,²⁹ and, on the other hand, their computational cost restricts their use to medium-size systems. Thus, CASPT2 and RASPT2 methods were rarely used to study the excited states of phosphors, see their application for, e.g., Pt(thpy)₂³⁰ and for a Ru(II)bipyridyl complex.³¹ Promisingly, the use of the multireference *ab initio* density matrix renormalization group (DMRG-CASPT2) approach, may permit the treatment of larger active spaces and larger TM complexes in the near future.³² Excited-state methods based on density functional theory (DFT), such as Δ SCF-DFT,³³ constricted variational DFT (CV-DFT)³⁴ and time-dependent DFT (TD-DFT),³⁵ are less costly, but are also less reliable, especially when compared

to the performance of DFT for ground-state properties of TM complexes. We discuss in this Perspective how ground state UDFT calculations can also provide important insights into photodeactivation pathways occurring on the lowest triplet excited state potential energy surface (PES). An alternative DFT-based method for electronically excited states makes use of Kohn-Sham orbitals in a multi-reference configuration interaction (MRCI) framework: in this DFT/MRCI method,³⁶ non-dynamic correlation effects are treated at the MRCI level whilst dynamic correlation effects are captured by the KS-DFT treatment. Recently, it was shown that DFT/MRCI is superior to TD-DFT approaches for the excited states of TMs.³⁷ DFT/MRCI generally provides the correct order of states and a balanced description of excited states of different character. By contrast, TD-DFT results are less balanced (difficulties at describing on the same footing excited states of different character) and functional dependent, particularly in the description of MLCT³⁷ as well as long-range CT states.³⁸ TD-DFT behaves erratically for MLCT states, which often have more local than CT character, with errors of up to 1 eV in some situations. In other cases these states are described with spectroscopic accuracy.³⁷ Despite the performances of the most widespread TD-DFT methods for organic dye and photochemistry,³⁹ their success with respect to the Δ SCF-DFT method for TMs was recently questioned by Ziegler et al, pointing out that these errors are likely originated due to the lack of orbital relaxation in adiabatic TD-DFT.⁴⁰ Among the different TD-DFT flavors, it is generally observed that hybrid exchange-correlation functionals with intermediate amounts of exact exchange, such as B3LYP (20%) or PBE0 (25%) outperform the rest of functionals for TMs,^{16,41} though errors are not systematic for all TM complexes so that it is difficult to develop general recommendations. Range-separated hybrid functionals, such as the CAM-B3LYP functional, are generally not recommended for TM complexes, especially for MLCT states.^{37,42} Clearly, future work should address all these important issues.

Spin-orbit effects are indispensable to interpret many spectroscopic phenomena, from ISC rates to zero-field splittings (ZFS). To reach tractable relativistic calculations including SOCs, the four-component Dirac equations are often reduced to 2-component approaches, such as the Douglas-Kroll-Hess (DKH)⁴³ or the zero-order regular approximation (ZORA)⁴⁴ Hamiltonians, which can be adapted to DFT, perturbation and wavefunction theory. SOC can be incorporated already in the orbital optimization step, such as in the self-consistent SOC-TDDFT method.⁴⁵ Alternatively, SOC can be included as a perturbation based on the scalar relativistic orbitals.⁴⁶ The progress in quasi-relativistic approaches extended the range of applications to a semi-quantitative interpretation of emission spectroscopy and photochemical reactivity, i.e. it is possible to compute ZFS and ISC and radiative rates. As shown in Ref. 47, for many TM complexes there is an important grade of admixture between pure spin states, which leads to mixed "spin-orbit" states. Not only the spectroscopic properties are modulated by the grade of admixture, but also the classical picture of pure (singlet, triplet or any other multiplicity) states may become meaningless.

Finally, recent progresses in mixed quantum-classical molecular dynamics methods, which permit the consideration of non-adiabatic effects between surfaces of different multiplicities,⁴⁸ should alleviate the path to perform excited-state dynamics calculations in phosphors. These simulations will enable one to reach time-dependent characterizations, as

shown for several Ru(II) polypyridyl complexes, though in these simulations, the SOCs are included in a qualitative manner.⁴⁹

III Photodeactivation dynamics of phosphors

This section follows a chronological order in the photodeactivation dynamics of phosphors and is organized as follows: In Section III.A, the ISC mechanisms are described. In Sections III.B and III.C the radiative and non-radiative mechanisms are presented, respectively.

A ISC mechanisms

The emission in Ir(III) and Pt(II) complexes is usually produced from triplet excited states. However, as discussed in the introduction, in some Pt(II) complexes, fluorescence might compete to ISC (i.e. $k_{ISC} \approx k_f$).¹¹ From an experimental viewpoint, three common characteristics can be generally used to identify fluorescence emission: small Stokes shifts, absence of photoluminescence quenching under aerated conditions and emission lifetimes in the nanosecond regime. Fluorescence-phosphorescence dual emissions have also been measured.⁵⁰ Chart 1 presents representative examples of a Pt(II) fluorophore (complex 1),⁵¹ a Pt(II) dual singlet-triplet emitter (complex 2),^{50a} and a cyclometalated Ir(III) dual triplet-triplet emitter (complex 3).⁵² The first two complexes bear extended π -conjugated ligands and their emissions are of ^{1,3}LLCT and/or ^{1,3}LC character, so that SO contributions on the involved emissive states are very small.

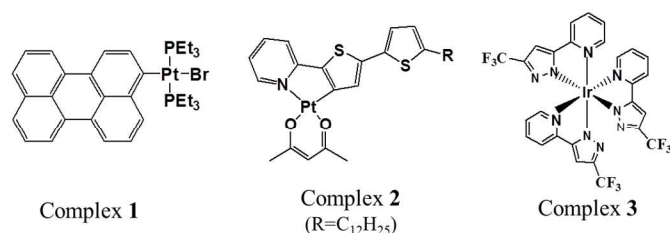


Chart 1. Chemical structure of complexes 1-3.

From this discussion it seems clear that an analysis of the ISC rates might provide important insights into the emissive behaviour of these chameleonic TM complexes. The ISC rate constants obey the empirical Fermi Golden rule expression

$$k_{ISC} = \frac{2\pi}{\hbar} \langle S_n | \hat{H}_{SO} | T_m \rangle^2 \times [FCWD], \quad (1)$$

where the bracket term stands for the SOCs between the involved S_n and T_m states and FCWD accounts for the Franck-Condon weighted density of states. Analogous expressions can be derived for other spin-states. Hence, from a computational viewpoint, the calculation of ISC rates requires in a first step the assignment of the main photodeactivation channels between the relevant S_n and T_m states (or other spin states) followed by an accurate estimation of i) SOC matrix elements, ii) energy difference between the electronic states, iii) vibrational frequencies, and iv) Huang-Rhys factors, which are related to the displacements between the excited state optimized geometries of the involved S_n and T_m states. Computing all parameters on Eq. (1) becomes rapidly prohibitive for large molecules. Instead of applying this time-independent approach, a time-dependent approach that alleviates the calculation of ISC

rates has been proposed.⁵³ The latter approach has been used to compute the ISC rates of the $[\text{Fe}(\text{bpy})_3]^{2+}$ complex (bpy=bipyridine), using accurate *ab initio* electronic structure calculations for relative energies, geometries and vibrational frequencies.⁵⁴ Based on these calculations the authors proposed an ultrafast photodeactivation cascade from the excited ^{1,3}MLCT band through different intermediate spin states (singlets, triplets and quintets) of MC or MLCT character. Relaxation to the lowest ⁵T_{2g} state occurs within 200 fs. The ultrafast relaxation can be understood in terms of the large SO and vibrational contributions to the computed k_{ISC} values, which ultimately roots on the proper alignment between spin states and the large SOCs between the metal-based singlet/triplet and triplet/quintet states. Recent time-resolved X-ray spectroscopy experiments provided additional information about the deactivation cascade and corroborated the computed ISC time-scales in $[\text{Fe}(\text{bpy})_3]^{2+}$.⁵⁵ A similar semi-quantitative approach to compute the ISC rates in TM emitters based on TD-DFT data has been recently proposed by Chou and coworkers.⁵⁶ Additionally, in the diplatinum PtPOP complex (see Introduction), a qualitative explanation of the relatively slow rate of ISC has also been proposed.¹⁰ The two lower-lying energy states in PtPOP, i.e. ¹A_{2u} and ³A_{2u} (both of $d\sigma^* \rightarrow p\sigma$ character), are energetically isolated from higher-lying states and well separated from each other. Their geometrical features are almost identical, resulting in very small Franck-Condon factors. Moreover, the direct spin-orbit interaction between the ¹A_{2u} and ³A_{2u} states is symmetry forbidden. All these facts lead to increased ISC time scales in PtPOP (up to 30 ps), despite the large Pt SOC constant. Gathering all this information, one can distinguish two clear, but qualitative, scenarios inducing sluggish ISC processes: i) ISC between low-energy isolated ^{1,3}LC and ^{1,3}LLCT states and ii) ISC between energetically isolated and well separated metal-based singlet and triplet states of same character/symmetry. In conflictive situations, e.g., when $k_{ISC} \approx k_f$, a quantitative approach to compute the ISC rates, like the one presented in Ref. 54, might be needed to assess whether emission is fluorescence- or phosphorescence-based.

Despite these previous considerations, in the vast majority of Ir(III) and Pt(II) complexes, emission is phosphorescence-based. Let us now turn our attention to their triplet-based photophysics, focusing on radiative and non-radiative deactivation pathways. The photoluminescence quantum yield (PLQY), which determines the internal efficiency of phosphors, is the ratio between the radiative (k_r) and non-radiative rates (k_{nr}).

$$\Phi_{phos} = \frac{k_r}{k_r + k_{nr}} \quad (2)$$

The PLQY is one of the most important factors in phosphor design. The PLQY depends on temperature and is one of the most important factors in phosphor design, as one wishes to favour the radiative processes over their non-radiative counterparts. As stated in the Introduction, some phosphors currently used in OLEDs reach efficiencies close to the unity of quantum yield at room temperature, for instance *fac*-Ir(ppy)₃ ($\Phi_{phos} = 0.97$).¹²

B Radiative deactivation mechanisms

Key information about the photophysical properties of phosphors can be obtained through low-temperature photoluminescence experiments. Yersin et. al have extensively

studied the emission characteristics of a series of TM phosphors at low temperatures using high-resolution and site-selective Shpol'skii spectroscopy – either with or without the application of high magnetic fields-,⁵⁷ e.g., for Pt(thpy)₂⁵⁸ and Ir(ppy)₃.⁵⁹ At near 0 K, the three substrates of the lowest triplet excited state (T₁) are resolved, since thermal population of the higher-lying substrates is not possible. Conversely, at ambient temperatures, the emission generally represents a thermalized decay from the different triplet substrates. Information regarding zero-field splittings (ZFS) can be derived from low temperature experiments. It is generally observed that the ZFS is a reliable parameter to characterize the size of the T₁→S₀ SOC and thus indirectly the amount of ³MLCT character of T₁. Usually, larger ZFS values are obtained for octahedral-like Ir(III) cyclometalated complexes [e.g., ca. 80 cm⁻¹ for Ir(ppy)₃] than for square-planar cyclometalated Pt(II) complexes [e.g., 16 cm⁻¹ for Pt(thpy)₂].⁵⁸ Importantly, the ZFS values can be computed in a relativistic framework that includes SOCs. Recently, Mori et al., showed a very good agreement between computed and measured ZFS values of 23 organometallic complexes - including Ir(ppy)₃ and Pt(thpy)₂ - with the help of SOC-TDDFT calculations.⁶⁰ Hence, on the basis of the ZFS values, a pure ³MLCT state is found to be responsible of the emission in the former complex whilst a mixed ³MLCT/³LC emission is found for Pt(thpy)₂. Computationally, the degree of ³MLCT/³LC mixing of the T₁ state also correlates to the spin density distribution at the metal atom, that is a less mixed ³MLCT character correlates to larger spin density at the metal atom. Gathering all this information, and according to the T₁→S₀ SOC estimates, the radiative drainage is more favoured in Ir(ppy)₃ than in Pt(thpy). However, the value of the T₁→S₀ SOC is not the only factor controlling the radiative efficiency. The phosphorescence radiative decay rates constants (k_r) from one of the three spin sublevels (indexed by *i*) of the involved emissive state (T_{em})[†] can be expressed as⁶¹

$$k_r^i = k_r(S_0, T_{em}^i) = \frac{4\alpha_0^3}{3t_0} \Delta E_{S-T}^3 \sum_{j \in \{x,y,z\}} |M_j^i|^2, \quad (3)$$

where ΔE_{S-T} is the transition energy, t₀ = (4πε₀)²/m_ee⁴, α₀ is the fine-structure constant and M_jⁱ is the *j* axis projection of the electric dipole transition moment between the ground state and the *i*th sublevel of the emissive triplet state, T_{em}. Note that individual phosphorescence rates for the three spin sublevels can only be determined under cryogenic conditions. As we stated above, at the high temperature limit, spin relaxation is usually fast and the triplet levels are almost equally populated. As a consequence, only weighted phosphorescence rates can be measured. Hence, phosphorescence rates are calculated according,

$$k_r = \frac{1}{3} \sum_{i=1}^3 k_r^i \quad (4)$$

By applying perturbation theory M_jⁱ can be expressed as¹⁷

$$M_j^i = \sum_{n=0}^{\infty} \frac{\langle S_0 | \hat{\mu}_j | S_n \rangle \langle S_n | \hat{H}_{SO} | T_{em}^i \rangle}{E(S_n) - E(T_{em})} + \frac{\langle S_0 | \hat{H}_{SO} | T_n \rangle \langle T_n | \hat{\mu}_j | T_{em}^i \rangle}{E(T_n) - E(S_0)}, \quad (5)$$

j ∈ {*x*, *y*, *z*},

where the nonzero contribution to the T_{em}→S₀ transition moment originates from the matrix elements of the electronic SOC operator (Ĥ_{SO}) including summation over intermediate triplet (T_n) and singlet (S_n) states. One can say that the T_{em}→S₀ transition borrows intensity from the spin-allowed S_n→S₀ and

T_{em}→T_n transitions. The sum-over-state expression, Eq (5), can also be solved using the quadratic response (QR) methodology.⁶² QR theory replaces Eq (5) by solutions of sets of linear equations, hence enabling the computation of radiative rates without need of truncation of the *n* values. This is of great numerical and theoretical advantage. The SOC operator might safely make use of a semi-empirical effective single-electron approximation.⁶³ Consequently, the first principles computation of the radiative rates using the QR TD-DFT calculations is nowadays a realistic task for relatively large TM complexes.⁶⁴ These calculations provided important insights into the radiative mechanisms of a series of Ir(III) cyclometalated complexes,⁶⁵ metaloporphyrines,⁶⁶ as well as Pt(II) cyclometalated complexes.¹⁴ Notably, the agreement between the computed and measured phosphorescence lifetimes is remarkable.¹⁷ Other semi-quantitative approaches have also been used to compute the k_r values of TM complexes.⁶⁷ Additionally, radiative rates have also been computed with SOC-TDDFT and perturbative SOC-TDDFT (pSOC-TDDFT) calculations for a set of 23 organometallic complexes for whose experimental radiative rates are available in the literature.⁶⁰

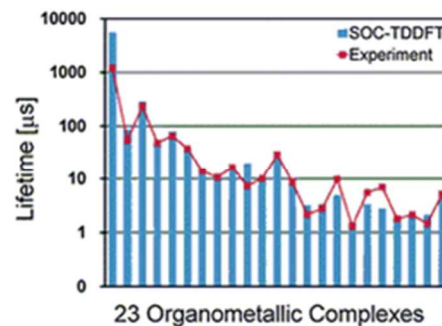


Figure 1. Comparison of the experimental and SOC-TDDFT (B3LYP/TZP) radiative lifetimes for 23 organometallic complexes. Reproduced from Ref. 60 with permission from the PCCP Owner Societies.

In Figure 1 the comparison of the experimental and SOC-TDDFT radiative lifetimes is shown. The agreement for most of the complexes is quite remarkable. As reported in Ref. 60, the less computationally demanding pSOC-TDDFT approach renders k_r values which are systematically underestimated with respect to the SOC-TDDFT values. The SOC-TDDFT approach yields the best agreement with experiment. Several groups have used different approaches to compute the k_r values of Ir(ppy)₃, from self-consistent SOC approaches to perturbative ones (i.e. QR and pSOC-TDDFT), and from using pseudopotentials to relativistic basis sets, e.g. Ref 60, 64b, 68, 69. The differences between the computed k_r values are not dramatic and in general a good agreement with the measured radiative lifetime is reported. However, other factors, e.g., the functional used in the TD-DFT calculations, the effect of solvation and the geometries employed, should be further assessed to develop a general and systematic approach to compute k_r.

In all these previous investigations, and leaving aside the fine-structure emission at cryogenic temperatures, it has been assumed that higher-lying triplet states are not involved in the radiative processes and that the radiative mechanisms are temperature-independent. However, there are many experimental evidences supporting temperature-dependent emissions from higher-lying states (see below). These experimental works are unfortunately not balanced by substantial computational contributions. According to the Kasha rule,⁷⁰ in the triplet manifold, there is fast decay to the T₁ state, from where emission likely occurs. The empirical Kasha rule was postulated before ultrafast spectroscopies were available. During

the past few years, these techniques permitted the capture of higher lying emissions in several molecular systems, i.e. from rhenium⁷¹ and diplatinum complexes¹⁰ to the C70 molecule.⁷² These findings represent mild violations of the Kasha rule as they are short lived. As we stated in Section III.A, another rather common feature in phosphor photochemistry is dual photoluminescence, with simultaneous emission from thermally equilibrated excited states.⁷³ Several Pt(II) and Ir(III) cyclometalated complexes show this behaviour.^{11,52} Both dual singlet-triplet⁵⁰ and triplet-triplet⁷⁴ emission were reported. A joint experimental and computational study of a dual phosphorescent Ir(III) complex,⁵² (**3** in Chart 1), found two triplet states to be responsible for its emission spectra: a low-lying ³MLCT/³LLCT state and a higher-lying ³MLCT/³LC state. At ambient temperatures (298 K) the spectrum is dominated by the Kasha-type ³MLCT/³LLCT emission. However, at lower temperatures (178 K) interconversion between both states is thermally not allowed, since there is a substantial activation barrier (ca. 2400 kcal/mol) for the ³MLCT/³LC → ³MLCT/³LLCT pathway. This prevents the relaxation to the lowest triplet state at low temperatures and thus breaches Kasha's rule. One of us recently reported the first computational evidence of a non-Kasha emissive behaviour for a Pt(II) cyclometalated complex at ambient temperatures and long timescales,¹⁴ see complex **4** in Figure 2a.

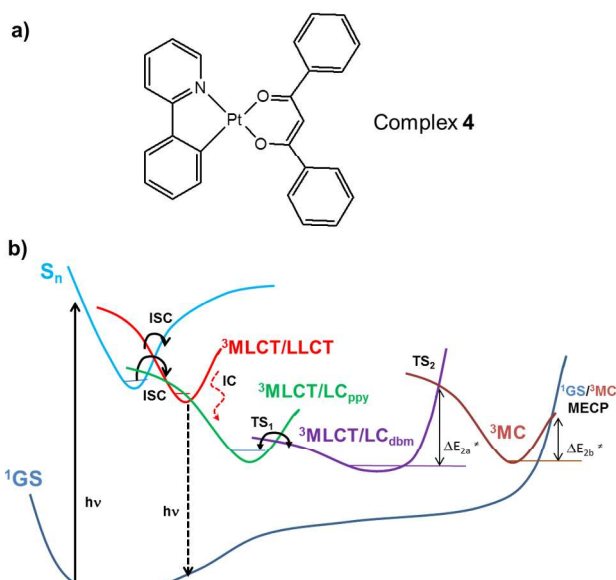


Figure 2. a) Chemical structure of the cyclometalated Pt(II) complex **4**. b) Schematic Jablonski diagram of complex **4**, including the lowest-energy triplet states involved in the photodeactivation pathways. Adapted with permission from Ref. 14. Copyright 2014 American Chemical Society.

Towards a full characterization of all possible photodeactivation pathways in complex **4**, the lowest triplet PES were explored with the help of UDFT and TD-DFT methods. The geometries of four different triplet excited states, i.e. ³MLCT/³LLCT, ³MLCT/³LC_{ppy}, ³MLCT/³LC_{dbm} and ³MC, and of relevant stationary points along the photodeactivation pathways, i.e., transition states and minimum energy crossing points (MECP), were fully optimized (see Figure 2b). The k_r values were computed from all possible emissive states with the help of QR TD-DFT calculations. As schematically shown in Figure 2b, the ³MLCT/³LC_{dbm} is the lowest-energy triplet excited state, that is the Kasha state. At ambient temperature the higher-lying states can be thermally populated (they are adiabatically located ca. 870 and 2270 cm⁻¹ above the Kasha

state). The k_r value arising from the higher-lying ³MLCT/³LLCT state is ca. two orders of magnitude larger than those arising from ³MLCT/³LC_{ppy} and ³MLCT/³LC_{dbm}. Consequently, if these states are thermally equilibrated, the radiative drainage will preferentially occur from the ³MLCT/³LLCT state. Indeed, the computed Δ SCF-PCM-DFT emission maximum from the ³MLCT/³LLCT state matches best the experimental one,⁷⁵ confirming the validity of these computational explorations. Gathering all this information, we feel that the design of estimators allowing to predict whether a complex will show dual photoluminescence, Kasha-emissive behaviour or non-Kasha behaviour at a given temperature will be of great interest to the phosphor and photophysics communities in the following years. To tackle this goal, we propose to use the following Boltzmann distribution

$$\frac{\phi(T_x)}{\phi(T_1)} = \frac{k_r(T_x)}{k_r(T_1)} e^{\left[\frac{-\Delta E(T_1 - T_x)}{k_B T} \right]}, \quad (6)$$

where the ratio of quantum yields of a higher-lying (T_x) and T_1 states is only determined by the ratio of their radiative rates, the barrier to populate the higher-lying state, i.e. $\Delta E(T_1 - T_x)$ and the temperature T . Generally, if the ratio is $<10^{-2}$, it will be difficult to observe the upper-lying emission (i.e. only the Kasha-like emission will be observed). Values $>10^{-2}$ imply non-Kasha emissions. Values in between these two values will lead to dual emission scenarios. Eq (6) can also be used to estimate the efficiency of TADF occurring in some Cu(I) and Ag(I) complexes,⁷⁶ under the assumption that the back ISC processes are fully allowed. In most TM complexes, the Kasha-emission is the most likely emissive scenario. Therefore, the computational strategy of optimizing the T_1 state still remains valid in most cases. Particularly challenging to model are complexes with many close-lying emissive triplet excited states, such as Complex **4**. Indeed, bidentate/tridentate/tetradentate Pt(II) complexes usually exhibit intricate photophysical properties, characterized by radiative decay rates and PLQY fluctuating when subtle variations of the electronic properties coupled to spin-orbit and vibronic contributions are made.⁷⁷ In turns, these variations are associated to a fine interplay of ligand substitution,⁷⁵ temperature⁵² and medium (solution/solid)²¹ which ultimately renders tunable radiative decay mechanisms. In short, the emissive properties of several phosphors are more complicated than expected, since the usual oversimplified picture of only the T_1 being responsible for the radiative decay mechanisms at ambient temperature is far from realistic for these TM complexes,^{14,77,78} as it has corroborated for complex **4**. These conclusions may help to explain the counterintuitive emissive behaviour in other Pt(II) cyclometalated complexes.⁷⁹

C Non-radiative deactivation pathways

Until now, we have focused on the radiative photodeactivation pathways. Now we focus on the non-radiative mechanisms. At ambient temperatures, one common competing mechanism to radiative photodeactivation is the thermal population of non-emissive ³MC states, which are commonly involved in these nonradiative decay channels,¹³ though there are exceptions.⁸⁰ These pathways increase the k_{nr} values and thus impair the PLQY, see Eq (2). Compared to Ru(II) complexes, the ³MC levels are usually destabilized in Ir(III) and Pt(II) complexes, due to the increased ligand field splitting for 5d metal atoms as compared to 4d metal atoms. Furthermore, when using

cyclometalating ligands there is a further destabilization of the 3MC states due to the strong field exerted by these ligands. If we compare Ir(III) and Pt(II) cyclometalated complexes, typically the first ones present more destabilized 3MC states, due to their quasi-octahedral environment and their higher oxidation state. Thus, as schematically depicted in Figure 2b, the 3MC state generally lies adiabatically higher than the emissive state.⁸¹ After photoexcitation, the system has in principle enough energy to populate the 3MC state. However, in the absence of dynamic simulations, which are still challenging for TM complexes, it is difficult to provide a theoretical estimate of the speed of dissipation of the excess energy and to determine if the barriers to populate the 3MC state constitute kinetic bottlenecks. As stated in Section III.A, experimental evidence points to ultrafast decay for many TM complexes to the T_1 state. Exemplarily, 8500 cm^{-1} (ca. 1 eV) of energy are dissipated in less than 300 fs within the manifold of electronic and vibrational levels in $[\text{Ru}(\text{bpy})_3]^{2+}$.⁸² Therefore, under these circumstances, a direct relaxation to the 3MC state (which will usually involve larger geometric distortions on its excited state PES) seems quite unlikely. Temperature-dependent lifetime measurements (77-300 K) for Ru(II)⁸³ and Ir(III) complexes^{13,84} provided relevant information about these deactivation channels. The rate constants and activation energies (ΔE^\ddagger) can be estimated by fitting the experimental data to an Arrhenius-like expression (Eq. 7),

$$\tau(T) = \frac{1}{k_r + \sum k_{nr}} = \frac{1}{k_r + k_1 + k_2 e^{(-\Delta E^\ddagger/k_B T)}} \quad (7)$$

Thus, and again leaving aside the temperature-dependent fine-structure emission at low temperatures (0-77 K), the excited-state lifetimes of these complexes depend on: i) k_r , ii) the non-radiative temperature-independent decay rate (k_1), which is associated with the Franck-Condon overlap between the S_0 and T_{em} vibrational wave functions and follows the energy gap law,⁸⁵ and finally iii) the strongly temperature-dependent non-radiative rate k_2 , which for these complexes is believed to be the principal non-radiative mechanism.¹² As demonstrated for several cyclometalated Ir(III) complexes,⁸⁴ additional components to Eq. (7), e.g., contributions associated to the population of higher-lying emissive states (see Section III.B), may be needed to fit the experimental data. Computational studies have provided very important insights into the temperature-dependent non-radiative photodeactivation pathways of Pt(II)^{14,86} and Ir(III) complexes.⁸⁷ The geometries of relevant stationary points along the non-radiative deactivation coordinate (see 3MC minimum, TS_2 and $^1GS/^3MC$ MECP in Figure 2b) need to be optimized to get a full adiabatic description of this pathway. As shown in Figure 2b, two rate-determining steps for these pathways are typically found for Ir(III) and Pt(II) cyclometalated complexes. One is the population of the 3MC well via the TS_2 structure. Thereafter, the $^1GS/^3MC$ surface crossing point is usually found to be easily accessible above the 3MC well. We underline the expected ultrafast nature of this ISC process, due to the very large SOCs between the 3MC and 1GS states. Therefore, the MECP is the most important funnel for the temperature-dependent non-radiative pathways. If enough thermal energy is available, the system will be able to pass these barriers and readily decay to the ground state. Importantly, the proximity of the $^1GS/^3MC$ MECP structure and the 3MC minimum ensures the high photostability of cyclometalated Pt(II) and Ir(III) complexes, as demonstrated by intrinsic reaction coordinate calculations starting from the $^1GS/^3MC$ MECP.⁸⁷ Once the

$^1GS/^3MC$ MECP is passed, the molecule will predominantly evolve to the 1GS geometry, though photodegradation is still a competitive pathway for some complexes, as recently reported by Thompson et. al.⁸⁸ As reported in Ref. 12 and 84 the measured ΔE_2^\ddagger activation energies range between 1600 cm^{-1} and 4800 cm^{-1} for a series of Ir(III) cyclometalated complexes, and these values are in fair good agreement with their computed counterparts. Importantly, the geometrical distortions along the $T_1 \rightarrow ^3MC \rightarrow \text{MECP}$ photodeactivation coordinate are different for Ir(III) complexes and Pt(II) complexes. Thus, the quasi-octahedral environment in Ir(III) complexes at the T_1 geometry usually evolves to a distorted trigonal bipyramidal environment at the 3MC and $^1GS/^3MC$ MECP geometries.^{12,87} On the contrary, the square-planar disposition in Pt(II) complexes at the T_1 geometry is conserved but stretched at the 3MC geometry, whilst the $^1GS/^3MC$ MECP geometry exhibits a tetrahedral-like distortion.¹⁴

In a nutshell, as demonstrated through these joint computational and experimental works, the role of the 3MC states and their associated barriers on the temperature-dependent non-radiative mechanisms are now demonstrated. Depending on the topology of the 3MC , T_1 and S_1 PES, two main different kinetic scenarios are possible: i) 3MC - T_1 pre-equilibration: in this case, the transition state (TS_2) for the $T_1 \rightarrow ^3MC$ conversion is energetically close to the $^1GS/^3MC$ MECP. This implies that the T_1 state is in equilibrium with the 3MC state before undergoing irreversible return to the ground state. In this case two activation barriers are kinetically relevant, i.e., the first for the $T_1 \rightarrow ^3MC$ conversion (ΔE_{2a}^\ddagger , see Figure 2b) and the second for the transition from the 3MC minimum to the $S_0/^3MC$ MECP (ΔE_{2b}^\ddagger in Figure 2b); ii) access to the 3MC well as rate-limiting step: here the activation barrier for the $^3MC \rightarrow S_0/^3MC$ MECP conversion is well below the ΔE_{2a}^\ddagger , so that the non-radiative deactivation kinetics is dominated by the activation barrier of the $T_1 \rightarrow ^3MC$ conversion. The computed energy profile of complex 4 follows the latter kinetic scenario (see Figure 2b).

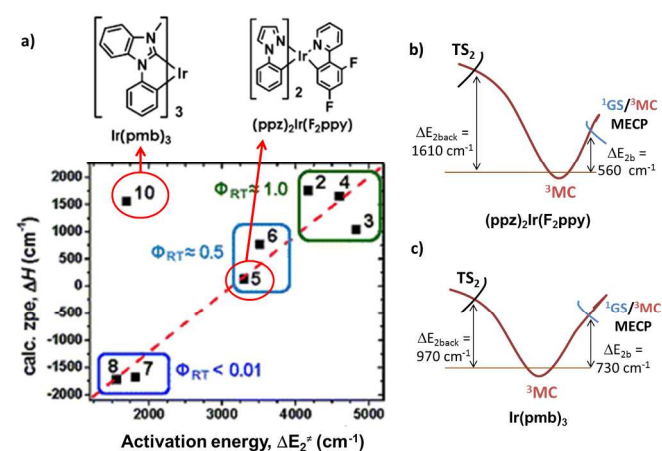


Figure 3. a) Plot of the activation energy (ΔE_2^\ddagger) vs ΔH for a series of Ir(III) complexes. The chemical structure of the herein studied compounds, $(\text{ppz})_2\text{Ir}(\text{F}_2\text{ppy})$ and $\text{Ir}(\text{pmb})_3$ are also shown. Adapted with permission from Ref. 12. Copyright 2014 American Chemical Society. b) and c) Computed energy profiles (UB3LYP/6-31G*) of the non-radiative pathways of $(\text{ppz})_2\text{Ir}(\text{F}_2\text{ppy})$ and $\text{Ir}(\text{pmb})_3$, respectively.

These kinetics speculations leads us to revisit the deactivation kinetics of a series of Ir(III) cyclometalated complexes reported in Ref. 12. In Figure 3a the measured activation energies (ΔE_2^\ddagger)

versus the calculated ΔH values are plotted. ΔH is a measure of the relative thermodynamic stability of the T_1 and 3MC states and, as shown in Ref. 12, is also an estimator of the PLQY (see the measured PLQY values at room temperature for different complexes in Figure 3a). As shown in Figure 3a, there is a linear correlation between ΔH and ΔE_2^\ddagger for the series of Ir(III) cyclometalated complexes, where $(ppz)_2Ir(F_2ppy)$ ($ppz=1$ -phenylpyrazole), $(F_2ppy=2$ -(4,6-difluorophenyl)pyridyl) belongs to this series. However, the $Ir(pmb)_3$ ($pmb=1$ -phenyl-3-methylbenzimidazolyl) complex, which bears a carbene ligand, does not follow the trend on ΔH , PLQY and ΔE_2^\ddagger . We have studied the temperature-dependent non-radiative mechanisms in $(ppz)_2Ir(F_2ppy)$ and $Ir(pmb)_3$ to shed some light into their different kinetic behaviour. The computational methodology to obtain the energy profiles (see Figure 3b-c) is analogous to that described in Ref. 87. For $(ppz)_2Ir(F_2ppy)$, the activation barrier for the ${}^3MC \rightarrow T_1$ back-reaction is ca. 1050 cm^{-1} above the barrier to overcome the ${}^1GS/{}^3MC$ MECP structure. Thus, once the 3MC well is populated in $(ppz)_2Ir(F_2ppy)$, it will likely undergo irreversible return to the ground state. On the contrary, in the case of $Ir(pmb)_3$, the activation barrier for the back-reaction lies only ca. 240 cm^{-1} above the ΔE_{2b}^\ddagger . Thus, for this carbene-based compound a pre-equilibrated 3MC - T_1 scenario is obtained. These calculations helped us to rationalize the different photodeactivation kinetics of $Ir(pmb)_3$ and its significant PLQY despite its low ΔE_2^\ddagger value. During the past years, similar kinetic considerations were also postulated by Meyer et al. for Ru(diimine) complexes through an analysis of their temperature-dependent experimental data.⁸⁹ The recent computational studies have deciphered the non-radiative deactivation pathways, and concomitantly they have corroborated the kinetic models proposed few years ago. In short, and as shown for this series of Ir(III) complexes, the inclusion of kinetic considerations in phosphor design is of great importance.

Conclusions and future work

The above selected examples were meant to illustrate some recent *ab initio* and DFT works performed to unveil photodeactivation pathways in phosphors. These computational studies provided important insights into their photophysical and photochemical properties, some of which are elusive to experiments. Special attention should be put to correctly interpret: i) the temperature-dependent photoluminescent data; and ii) the unusual photophysics of several Ir(III) and Pt(II) complexes, leading to dual photoluminescence and Non-Kasha emissive behaviour. In the upcoming years, the continuous progresses in quantum chemical and reaction dynamics methods will enable to obtain time-resolved information and quantum yields for all possible photodeactivation pathways. Towards these ultimate aims, accurate theoretical estimates for excited states energies, geometries, vibrational frequencies and SOCs are needed. The current *ab initio* and DFT machinery is still not systematically accurate enough for the excited states of TM complexes. Therefore, further theoretical developments are needed. In this regard, particularly promising are hybrid methods combining wave function and density functional theories. This progress should be complemented with further developments in experimental techniques. For instance, as detailed for $[Fe(bpy)_3]^{2+}$, ultrafast X-ray spectroscopies may provide more information about the charge, spin and structural dynamics of molecular systems.⁹⁰ Joint experimental and computational efforts will be needed to address future research in phosphors design, such as the fine

interplay with the environment in the OLED's emissive layer or addressing the competing photodeactivation pathways opened up in the condensed phase due to aggregation, i.e. TTA processes, which determine "roll-off" in OLEDs.

Acknowledgements

D.E. acknowledges the European Research Council (ERC) for his post-doctoral grant (Marches – 278845). D.J. acknowledges the European Research Council (ERC) and Région des Pays de La Loire for financial support in the framework of a Consolidator Grant (Marches – 278845) and the LUMOMAT RFI project, respectively.

Notes and references

^a Chimie Et Interdisciplinarité, Synthèse, Analyse, Modélisation (CEISAM), UMR CNRS no. 6320, BP 92208, Université de Nantes, 2, Rue de la Houssinière, 44322 Nantes, Cedex 3, France. E-mail: daniel.escudero@univ-nantes.fr

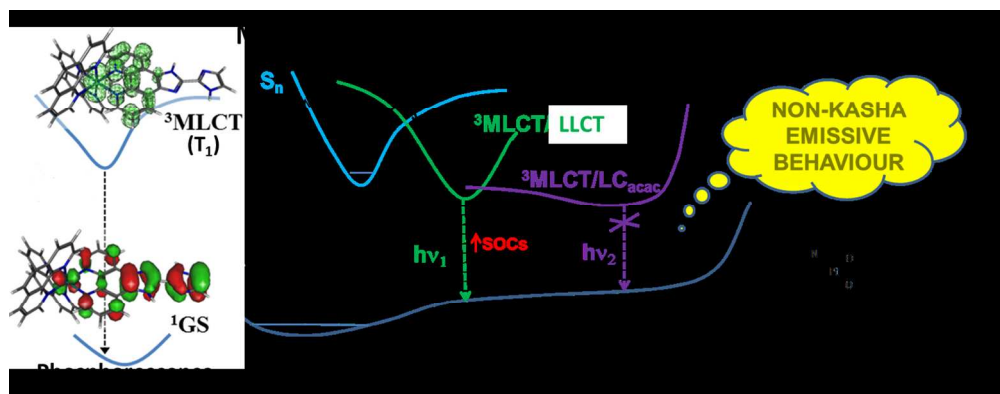
^b Institut Universitaire de France (IUF), 103 blvd St Michel, 75005 Paris Cedex 05, France.

† In the following, to get a more general expression we substitute T_1 for T_{em} .

- a) C. W. Tang and S. A. Vanslyke, *Appl. Phys. Lett.*, 1987, **51**, 913; b) J. H. Burroughes, D. D. C. Bradley, A. R. Brown, R. N. Marks, K. Mackay, R. H. Friend, P. L. Burns and A. B. Holmes, *Nature*, 1990, **347**, 539.
- H. Uoyama, K. Goushi, K. Shizu, H. Nomura and C. Adachi, *Nature*, 2012, **492**, 234.
- C. Adachi, M. A. Baldo, M. E. Thompson and S. R. Forrest, *J. Appl. Phys.*, 2001, **90**, 5048.
- A. F. Rausch, H. H. H. Homeier and H. Yersin, *Top. Organomet. Chem.*, 2010, **29**, 193.
- C. Murawski, K. Leo and M. C. Gather, *Adv. Mater.*, 2013, **25**, 6801.
- S. Reineke and M. A. Baldo, *Phys. Status Solidi A*, 2012, **12**, 2341.
- M. Chergui, *Dalton Trans.*, 2012, **41**, 13022.
- a) G. J. Hedley, A. Ruseckas and I. D. W. Samuel, *J. Phys. Chem. A*, 2009, **113**, 2; b) K. C. Tang, K. L. Liu and I. C. Chen, *Chem. Phys. Lett.*, 2004, **386**, 437.
- H. Yersin, A. F. Rausch, R. Czerwieniec, T. Hofbeck and T. Fischer, *Coord. Chem. Rev.*, 2011, **255**, 2622.
- R. M. van der Veen, A. Canizzo, F. van Mourik, A. Vlcek and M. Chergui, *J. Am. Chem. Soc.*, 2011, **133**, 305.
- Y. Y. Chia and M. G. Tay, *Dalton Trans.*, 2014, **43**, 13159.
- T. Sajoto, P. I. Djurovich, A. B. Tamayo, J. Oxgaard, W. A. Goddard III and M. E. Thompson, *J. Am. Chem. Soc.*, 2009, **131**, 9813.

- ¹³ L. Yang, F. Okuda, K. Kobayashi, K. Nozaki, Y. Tanabe, Y. Ishii and M. A. Haga, *Inorg. Chem.*, 2008, **47**, 7154.
- ¹⁴ D. Escudero and W. Thiel, *Inorg. Chem.*, 2014, **53**, 11015.
- ¹⁵ L. González, D. Escudero and L. Serrano-Andrés, *ChemPhysChem*, 2012, **13**, 28.
- ¹⁶ C. Daniel, *Coord. Chem. Rev.*, 2015, **282**, 19.
- ¹⁷ B. Minaev, G. Baryshnikov and H. Agren, *Phys. Chem. Chem. Phys.*, 2014, **16**, 1719.
- ¹⁸ M. Mauro, G. De Paoli, M. Otter, D. Donghi, G. D'Alfonso and L. De Cola, *Dalton Trans.*, 2011, **40**, 12106.
- ¹⁹ D. L. Rochester, S. Develay, S. Zalis and J. A. Gareth Williams, *Dalton Trans.*, 2009, 1728.
- ²⁰ T. Kayano, S. Takayasu, K. Sato and K. Shinozaki, *Chem. Eur. J.*, 2014, **20**, 16583.
- ²¹ a) Y. Nishiuchi, A. Takayama, T. Suzuki and K. Shinozaki, *Eur. J. Inorg. Chem.*, 2011, **2011**, 1815; b) A. Amar, H. Meghezzi, J. Boixel, H. Le Bozec, V. Guerchais, D. Jacquemin and A. Boucekkine, *J. Phys. Chem. A*, 2014, **118**, 6278; c) D. Kim and J.-L. Brédas, *J. Am. Chem. Soc.*, 2009, **131**, 11371; d) Y. Wu, H.-Z. Sun, H.-T. Cao, H.-B. Li, G.-G. Shan, Y.-A. Duan, Y. Geng, Z.-M. Su and Y. Liao, *Chem. Commun.*, 2014, **50**, 10986.
- ²² a) G. Cheng, S. C. F. Kui, W.-H. Ang, M.-Y. Ko, P.-K. Chow, C.-L. Kwong, C.-C. Kwok, C. Ma, X. Guan, K.-H. Low, S.-J. Su and C.-M. Che, *Chem. Sci.*, 2014, **5**, 4819; b) K. Li, G. Cheng, C. Ma, X. Guan, W.-M. Kwok, Y. Chen, W. Lu and C.-M. Che, *Chem. Sci.*, 2013, **4**, 2630.
- ²³ R. Liu, A. Azenkeng, D. Zhou, Y. Li, K. D. Glusac and W. Sun, *J. Phys. Chem. A*, 2013, **117**, 1907.
- ²⁴ a) X. Zhang, J.-Y. Wang, J. Ni, L.-Y. Zhang and Z.-N. Cheng, *Inorg. Chem.*, 2012, **51**, 5569; b) S. C. F. Kui, P. K. Chow, G. S. M. Tong, S.-L. Lai, G. Cheng, C.-C. Kwok, K.-H. Low, M. Y. Ko and C.-M. Che, *Chem. Eur. J.*, 2013, **19**, 69.
- ²⁵ J. Zhao, S. Ji and H. Guo, *RSC Adv.*, 2011, **1**, 937.
- ²⁶ K. Andersson, P.-A. Malmqvist and B. O. Roos, *J. Chem. Phys.*, 1992, **96**, 1218.
- ²⁷ P.-A. Malmqvist, K. Pierloot, A. R. M. Shahi, J. C. Cramer and L. Gagliardi, *J. Chem. Phys.*, 2008, **128**, 204109.
- ²⁸ K. Pierloot, *Int. J. Quantum Chem.*, 2011, **111**, 3291.
- ²⁹ K. Pierloot, *Mol. Phys.*, 2003, **101**, 2083.
- ³⁰ K. Pierloot, A. Ceulemans, M. Merchán and L. Serrano-Andrés, *J. Phys. Chem. A*, 2000, **104**, 4374.
- ³¹ D. Escudero and L. González, *J. Chem. Theory and Comput.*, 2012, **8**, 203.
- ³² K. H. Marti and M. Reiher, *Phys. Chem. Chem. Phys.*, 2011, **13**, 6750.
- ³³ a) D. Gunnarsson and B. I. Lundqvist, *Phys. Rev. B*, 1976, **13**, 4272; b) T. Ziegler, *Chem. Rev.*, 1991, **91**, 651.
- ³⁴ T. Ziegler, M. Seth, M. Krykunov, J. Autschbach and F. Wang, *J. Chem. Phys.*, 2009, **130**, 154102.
- ³⁵ a) E. Runge and E. K. U. Gross, *Phys. Rev. Lett.*, 1984, **12**, 997; b) M. Petersilka, U. J. Gossmann and E. K. U. Gross, *Phys. Rev. Lett.*, 1996, **76**, 1212.
- ³⁶ S. Grimme and M. Waletzke, *J. Chem. Phys.*, 1999, **111**, 5645.
- ³⁷ D. Escudero and W. Thiel, *J. Chem. Phys.*, 2014, **140**, 194105.
- ³⁸ A. Dreuw and M. Head-Gordon, *J. Am. Chem. Soc.*, 2014, **126**, 4007.
- ³⁹ a) A. D. Laurent and D. Jacquemin, *Int. J. Quantum Chem.*, 2013, **113**, 2019; b) A. D. Laurent, C. Adamo and D. Jacquemin, *Phys. Chem. Chem. Phys.*, 2014, **16**, 14334.
- ⁴⁰ H. R. Zhekova, M. Seth and T. Ziegler, *Int. J. Quantum Chem.*, 2014, **114**, 1019.
- ⁴¹ A. Gabrielsson, S. Zalis, P. Matousek, M. Towrie and A. Vleck Jr., *Inorg. Chem.*, 2004, **43**, 7380.
- ⁴² T. Le Bahers, E. Brémond, I. Ciofini and C. Adamo, *Phys. Chem. Chem. Phys.*, 2014, **16**, 14435.
- ⁴³ a) B. A. Hess, *Phys. Rev. A*, 1985, **32**, 756; b) B. A. Hess, *Phys. Rev. A*, 1989, **39**, 6016.
- ⁴⁴ a) E. van Lenthe, E. J. Baerends and J. G. Snijders, *J. Chem. Phys.*, 1993, **99**, 4597; b) E. van Lenthe, E. J. Baerends and J. G. Snijders, *J. Chem. Phys.*, 1994, **101**, 9783.
- ⁴⁵ F. Wang, T. Ziegler, E. Van Lenthe, S. J. A. Van Gisbergen and E. J. Baerends, *J. Chem. Phys.*, 2005, **122**, 204103.
- ⁴⁶ F. Wang and T. Ziegler, *J. Chem. Phys.*, 2005, **123**, 154102.
- ⁴⁷ R. Bakova, M. Chergui, C. Daniel, A. Vleck Jr., S. Zalis and C. Daniel, *Coord. Chem. Rev.*, 2011, **255**, 975.
- ⁴⁸ a) M. Richter, P. Marquetand, J. González, I. Sola and L. González, *J. Chem. Theory Comput.*, 2011, **7**, 1082; b) L. Martínez, I. Corral, G. Granucci and M. Persico, *Chem. Sci.*, 2014, **5**, 1336.
- ⁴⁹ I. Tavernelli, B. F. E. Curchod and U. Rothlisberger, *Chem. Phys.*, 2011, **391**, 101.
- ⁵⁰ a) D. Kozhevnikov, V. N. Kozhevnikov, M. Z. Shafikov, A. M. Prokhorov, D. W. Bruce and J. A. Gareth Williams, *Inorg. Chem.*, 2011, **50**, 3804; b) A. C. Durrell, G. E. Keller, Y.-C. Lam, J. Sýkora, A. Vlcek Jr and H. B. Gray, *J. Am. Chem. Soc.*, 2012, **134**, 14201; c) M. Z. Hudson, S.-B. Zhao, R.-Y. Wang and S. Wang, *Chem. Eur. J.*, 2009, **15**, 6131.
- ⁵¹ S. Lentijo, J. A. Miguel and P. Espinet, *Inorg. Chem.*, 2010, **49**, 9169.
- ⁵² Y.-S. Yeh, Y.-M. Cheng, P.-T. Chou, G.-H. Lee, C.-H. Yang, Y. Chi, C.-F. Shu, C.-H. Wang, *ChemPhysChem*, 2006, **7**, 2294.

- ⁵³ M. Etinski, J. Tatchen and C. M. Marian, *J. Chem. Phys.*, 2011, **134**, 154105.
- ⁵⁴ C. Sousa, C. de Graaf, A. Rudavskiy, R. Broer, J. Tatchen, M. Etinski and C. M. Marian, *Chem. Eur. J.*, 2013, **19**, 17541.
- ⁵⁵ W. Zhang, R. Alonso-Mori, U. Bergmann, C. Bressler, M. Chollet, A. Galler, W. Gawelda, R. G. Hadt, R. W. Hartsock, T. Kroll, K. S. Kjær, K. Kubicek, H. T. Lemke, H. W. Liang, D. A. Meyer, M. N. Nielsen, C. Purser, J. S. Robinson, E. I. Solomon, Z. Sun, D. Sokaras, T. B. van Driel, G. Vankó, T.-S. Weng, D. Zhu and K. Gaffney, *Nature*, 2014, **509**, 345.
- ⁵⁶ E. Y.-T. Li, T.-Y. Jiang, Y. Chi and P.-T. Chou, *Phys. Chem. Chem. Phys.*, 2014, **16**, 26184.
- ⁵⁷ H. Yersin, *Top. Curr. Chem.*, 2004, **241**, 1.
- ⁵⁸ H. Yersin and D. Dongues, *Top. Curr. Chem.*, 2001, **214**, 81.
- ⁵⁹ W. J. Finkenzeller and H. Yersin, *Chem. Phys. Lett.*, 2003, **337**, 299.
- ⁶⁰ K. Mori, T. P. M. Goumans, E. van Lenthe and F. Wang, *Phys. Chem. Chem. Phys.*, 2014, **16**, 14523.
- ⁶¹ S. P. McGlynn, T. Azumi and M. Kinoshita, *Molecular Spectroscopy of the Triplet State*, Prentice Hall, Engelwood Cliffs, New Jersey, 1969.
- ⁶² a) I. Tunnel, Z. Rinkevicius, P. Salek, O. Vahtras and H. Agren, *J. Phys. Chem.*, 2003, **119**, 11024; b) H. Agren, O. Vahtras and H. Agren, *Adv. Quantum Chem.*, 1996, **27**, 71.
- ⁶³ S. Koseki, M. Schmidt and M. Gordon, *J. Phys. Chem.*, 1990, **96**, 10678.
- ⁶⁴ a) B. Minaev and H. Agren, *Chem. Phys.*, 2005, **315**, 215; b) E. Jansson, B. Minaev, S. Schrader and H. Agren, *Chem. Phys.*, 2007, **333**, 157; c) O. Vahtras, H. Agren, J. Jorgensen, H. J. Aa. Jensen, T. Helgaker and J. Olsen, *J. Chem. Phys.*, 1992, **97**, 9178.
- ⁶⁵ a) X. Li, B. Minaev, H. Agren and H. Tian, *Eur. J. Inorg. Chem.*, 2011, **2011**, 2517; b) X. Li, B. Minaev, H. Agren and H. Tian, *J. Phys. Chem. C*, 2011, **115**, 20724.
- ⁶⁶ B. Minaev, E. Jansson, H. Agren and S. Schrader, *J. Chem. Phys.*, 2006, **125**, 234704.
- ⁶⁷ a) D. Escudero, B. Happ, A. Winter, M. D. Hager, U. S. Schubert and L. González, *Chem. Asian J.*, 2012, **7**, 667; b) G. S.-M. Tong and C.-M. Che, *Chem. Eur. J.* 2009, **15**, 7225; c) Z. A. Siddique, Y. Yamamoto, T. Ohno and K. Nozaki, *Inorg. Chem.*, 2003, **42**, 6366.
- ⁶⁸ K. Nozaki, *J. Chin. Chem. Soc.*, 2006, **53**, 101.
- ⁶⁹ H. Sasabe, J. Takamatsu, T. Motoyama, S. Watanabe, G. Wagenblast, N. Langer, O. Molt, E. Fuchs, C. Lennartz and J. Kido, *Adv. Mater.*, 2010, **22**, 5003.
- ⁷⁰ M. Kasha, *Discuss. Faraday Soc.*, 1950, **9**, 14.
- ⁷¹ A. Canizzo, A. M. Blanco-Rodríguez, A. El Nahhas, J. Sebera, S. Zalis, A. Vlcek, Jr. and M. Chergui, *J. Am. Chem. Soc.*, 2008, **130**, 8967.
- ⁷² A. Sassara, G. Zerza, and M. Chergui, *J. Phys. Chem. A*, 1998, **102**, 3072.
- ⁷³ a) K. K.-W. Lo, K. Y. Zhang, S.-K. Leung and M.-C. Tang, *Angew. Chem. Int. Ed.*, 2008, **47**, 2213; b) S. Ladouceur, L. Donato, M. Romain, B. P. Mudraboyina, M. B. Johansen, J. A. Wisner and E. Zysman-Colman, *Dalton Trans.*, 2013, **42**, 8838.
- ⁷⁴ Y. You, S. Lee, T. Kim, K. Ohkubo, W.-S. Chae, S. Fukuzumi, G.-J. Jhon, W. Nam and S. J. Lippard, *J. Am. Chem. Soc.*, 2011, **133**, 18328.
- ⁷⁵ J. Liu, C.-J. Yang, Q.-Y. Cao, M. Xu, J. Wang, H.-N. Peng, W.-F. Tan, X.-X. Lü and X.-C. Gao, *Inorg. Chim. Acta.*, 2009, **362**, 575.
- ⁷⁶ H. Yersin, M. J. Leidl and R. Czerwieńiec, *Proc. SPIE*, 2014, **9183**, 91830N-1.
- ⁷⁷ C. Gourlaouen and C. Daniel, *Dalton Trans.*, 2014, **43**, 17806.
- ⁷⁸ V. Anbalagan and T. S. Srivastava, *Polyhedron*, 2004, **23**, 3173.
- ⁷⁹ A. Bossi, A. F. Rausch, M. J. Leidl, R. Czerwieńiec, M. T. Whited, P. I. Djurovich, H. Yersin, and M. E. Thompson, *Inorg. Chem.*, 2013, **52**, 12403.
- ⁸⁰ Y. Liu, P. I. Djurovich, R. Haiges and M. E. Thompson, *Polyhedron*, 2014, **84**, 136.
- ⁸¹ R. D. Costa, E. Ortí, H. J. Bolink, F. Monti, G. Accorsi and N. Armaroli, *Angew. Chem. Int. Ed.*, 2012, **51**, 8178.
- ⁸² A. Cannizzo, F. van Mourik, W. Gawelda, G. Zgrablic, C. Bressler and M. Chergui, *Angew. Chem. Int. Ed.*, 2006, **45**, 3174.
- ⁸³ a) S. H. Wadman, M. Lutz, D. M. Tooke, A. L. Speck, F. Hartl, R. W. A. Havenith, G. P. M. van Klink and G. van Kooten, *Inorg. Chem.*, 2009, **48**, 1887; b) A. C. Benniston, G. Chapman, A. Harriman, M. Mehrabi and C. A. Sams, *Inorg. Chem.*, 2004, **43**, 4227.
- ⁸⁴ R. D. Costa, F. Monti, G. Accorsi, A. Barbieri, H. J. Bolink, E. Ortí and N. Armaroli, *Inorg. Chem.*, 2011, **50**, 7229.
- ⁸⁵ J. S. Wilson, N. Chawdhury, M. R. A. Al-Mandhary, M. Younus, M. S. Khan, P. R. Raithby, A. Köhler and R. H. Friend, *J. Am. Chem. Soc.*, 2001, **123**, 9412.
- ⁸⁶ W. H. Lam, E. S.-H. Lam and V. W.-W. Yam, *J. Am. Chem. Soc.*, 2013, **135**, 15135.
- ⁸⁷ D. Escudero, E. Heuser, R. J. Meier, M. Schäferling, W. Thiel and E. Holder, *Chem. Eur. J.*, 2013, **19**, 15639.
- ⁸⁸ M. J. Jurow, A. Bossi, P. I. Djurovich and M. E. Thompson, *Chem. Mater.*, 2014, **26**, 6578.
- ⁸⁹ B. Durham, J. V. Caspar, J. K. Nagle and T. J. Meyer, *J. Am. Chem. Soc.*, 1982, **104**, 4803.
- ⁹⁰ M. Chergui, *Faraday Discuss.*, 2014, **171**, 11.



260x102mm (150 x 150 DPI)